A global method of generating action potentials and EEG oscillations in a topological surface network

Model Predictions and Speculations

Siddhartha Sen (Email: sen1941@gmail.com)
Centre for Research in Adaptive Nanostructures and Nanodevices,
School of Physics, Trinity College Dublin, Ireland

Acknowledgment

I would like to thank Samik Sen for producing all the EEG waveform Gnuplots. Mike Coey and Mani Ramaswami for encouragement, Tomas Ryan, Maurizio Pezzoli and David Muldowney for collaborating with me on the soliton pulse work summarized and for numerous discussions. This research did not receive any specific grant from funding agencies in the public, commercial or not-for-profit sector.

Abstract

We prove that it is possible to construct a mathematical surface network that exactly captures the topological connectivity architecture of any hypothetical brain connectome. The surface has electrons. Local surface deformations are universal input signals of the network. They have signal specific parameters and change the topology of the subunit to that of a sphere, to produce a wide variety of output signals that include one dimensional soliton pulses, transient localized excitations and EEG-like surface waveforms. Thus the two topological numbers of the subunit,g that reflects its connectivity and W that reflects topological arrangements of the surface electron spin magnets are reduced to zero, the topological numbers of the sphere. Both of these topological numbers as well as the signal specific deformation parameters are carried away by the soliton pulses. The charged moving soliton transfers the signal specific distortion parameters they carry to create a non-transient helical electron spin-magnet alignment, a memory trace, with a theoretically estimated specific frequency label. The structure is created by the magnetic field generated by the charged moving solitons. A dynamical principle that requires that all input signals and responses to them must respect the mathematical properties of the network surface is used to derive all results. Predictions regarding the the frequencies and shapes of the EEG like waveforms are made that are consistent with observations. A theoretical interpretation of a complex sequence of EEG events observed in deep sleep, where it is assumed that signal blocking events play a key role,is carried out using a Greens function formula derived for calculating the response of EEG waveforms to input signals. Memory retrieval is shown to have quantum computer like features.

keywords: memory retrieval, solitons , blocking excitations, surface waveforms, K-complexes, sleep-spindles, sharp-wave ripples, attention

Introduction

It is widely accepted that the electrical activity of the brain in the form of a variety of one dimensional voltage pulses, action potentials, localized transient oscillations and ever present surface oscillations in five frequency bands, EEG waveforms, play in role in functioning of the brain.

In this paper we demonstrates that it is mathematically possible to produce all of these brain-like excitations by local topological deformations on a specially chosen surface network that has surface electrons. The network we prove exactly captures the complex topological connectivity properties of any hypothetical brain connectome. Thus the scheme shows that the form of the network, its topological connectivity, is directly related to its function as a signal generating system. The presence of surface electrons is essential for both signal generation and, as we will explain, memory storage.

We first prove that such a network exists. A connectome is a network of lines (axons) and junction points (soma) spread over three dimensions. By replacing each line by a tube and each junction point by a junction region a surface representation of the connectome, again spread over three dimension can be constructed. The mathematical theorem on the topological classification of surfaces,(Munkres,2014) tells us that such a surface is topologically equivalent to a sphere with g handles (Fig1)or an orderly arrangement of g donuts (Fig 3). The number g is called the genus of the surface and the theorem tells us that this one number completely captures the topological connectivity of a compact orientable surface. We should point out that the geometrical arrangements of anatomical units are no longer preserved in the topological description but all connectivity information is preserved.

The procedure described creates a surface with topological properties. If we further require that the surface, an arrangement of g donuts, is smooth then it is mathematical surface called a genus g Riemann surface. A Riemann surface is a clever geometrical way of representatinf any polynomial equation $P(z, w)$ of two complex variables discovered by Riemann. There are numerous Riemann surfaces that can represent a genus g surface. Surprisingly it is possible to prove that only a special subclass of Riemann surfaces (Arberello,2001) can produce brain like excitations by special local surface deformations provided the surface has electrons. Thus we select such a Riemann surface for our surface network. It is described by the polynomial equation $w^2 = P(z)$ with $P(z) = \Pi_{i=1}^{(2g+2)}(z - x_i)$, called the hyperelliptic equation.

Surface electrons introduced give an additional topological number W to the surface network which reflects the presence of topologically inequivalent arrangements of linked electron spin magnets that are possible.

To relate form to function we introduce a dynamical principle that requires that all surface deformation, input signals and output signal responses to them must respect the mathematical structure of the Riemann surface introduced. This means the form of system should be respected. We show that this principle is enough to derive all of our results.

The universal input signals of the network are local pinch deformations. These signals carry deformations specific to asignal and they reduce tube radii of a subunit to zero, in a wy shown in Fig 2 that changes the topology of the subunit to that of a sphere. In this way a wide variety of excitaions including one dimensional soliton pulses (Mumford,1987) can be generated by the subunit, provided surface electrons are present. Signal generation can be more precisly described as a process in which the topology numbers of the subunit changes from (g, W) to $(0, 0)$ and the excitations created carry away these topological numbers. The pinch deformations also contain signal specific deformation parameters. These too are carried away by the excitations. A genus g subunit creates g soliton pulses.

To make this point clear we write out the structure of the j^{th} soliton pulse when g pulses are produced. If the soliton is travelling along the x direction, it has the structure $e^{-i\pi W}V_j(A_jx - B_jt + C_j), j = 1, 2, ..g$ where $A_j, B_j, C_j)$ are signal specific pinch deformation parameters (sen,2022) and W the surface spin magnet topology number . From this expression we can determine the soliton speed. For our discussions the speed of the charges carried by the soliton and its form are important. As these moving charges generate a magnetic field (Jackson,1962) that acts on the surface spin magnets, aligning them to form a static memory trace of the pinch deformation, that is the input signal, information. Thus we need to relate the voltage pulse signals to charges. This is done by using the equation of electromagnetism,$\nabla_x^2 V_j = \rho_j$ where $\rho_j(A_jx - B_jt + C_j)$ Is the charge density. The soliton potential is found to have an exponential form,(Mumford,1987). Thus we get $V_j = \frac{\rho_j}{A_j^2}$. Thus the speed of the soliton $v_j = \frac{B_j}{A_j^3}$ depends on the pinch deformation parameters:it is signal dependent.

To simplify our analysis we replace ρ_j by $\frac{Q_j}{\Delta_j}$ where Δ_j is an effective width of the pulse. For N moving soliton pulses the magnetic field created by them $\vec{B}$is given by $\vec{B} = \sum_{j=1}^{N} \vec{B}_j$. If the j^{th} soliton moves with speed v_j along the z-axis ,the magnetic field at any point is tangential to and constant on any surface point on a circle of radius r from the axis along which the soliton is moving. Thus the field is a helical field circling round a tube of radius r, with magnitude $B_j = \frac{Q_j v_j}{cr^2}$, where c is the speed of light in the medium.(Jackson,1962). We thus write the transient helical field in terms of coordinates as $B\cos(\frac{2\pi z_j}{L}), B\sin(\frac{2\pi z_j}{L}, z_j = v_jt$, where L is a loop length travesred by the pulse. We next turn to calculate the static helical structure of spin magnets formed by spin magnets that are in the helical pathway of the magnetic field, and also calculte their excitation frequency.

Helical Static Spin-Magnet Structures and Excitation Frequencies

The transient magnetic field moving on the surface in a helical way, as described, acts on the surface electron spin magnets, $\vec{s}$ on its path and alignes them via the quantum interaction $H = \mu\vec{B}.\vec{s} = \mu\vec{B}\vec{\sigma}$, where $\vec{\sigma}$ are Pauli spin matrices that describe the spin magnet properties of an electron, and μ is the Bohr magneton (Landau,1977). The interaction is a quantum operator. The Pauli matrices act on spin vectors that have two componts a spin up and a spin down component with spin values $\pm\frac{1}{2}$. For an aligned spin we set the spin value to be $+\frac{1}{2}$. The interaction written down results in the formation of a static helical spin-magnet structure, a memory trace as we will show, while the natural excitation frequency of the structure is determined directly by the interaction H. Let us estimate this frequency. If we write the moving soliton pulse charge as $Q_j = N_j e$ then quantum theory tells us the natural excitation frequency of the system is given by $\omega_j = \frac{H}{\bar{h}} = \frac{\mu B}{\bar{h}}$ with $B = \frac{Q_j v_j}{cr^2} \approx N_j$,and $\bar{h}$ is Planck's constant. if we set $c \approx 10^9 cm/s.(Khurgin, 2010)$ and set $e \approx 10^{-10}, \mu \approx 10^{-19}, v_j \approx 10^3, \bar{h} \approx 10^{-27} r \approx 10^{-4} cm$ in CGS units. A quantum calculation is appropriate for electrons. Thus for a pulse carrying N_j units of electron charge, in the range $1 \leq N_j \leq 10^2$, will lead to the excitation frequencies of the static memory trace to be in the range $1 \leq \omega_j \leq 100$ Hz that overlap with observed EEG waveform frequencies.

We next determine the static helical spin magnet structure. A quantum calculation is needed to do this. The time evolution of a spin is described by the operator $U(t) = e^{-i\frac{Ht}{\bar{h}}}$, where $H = \mu\vec{B}.\vec{\sigma} = \mu\vec{n}.\vec{\sigma}B$ where we have written $\vec{B} = \vec{n}B$ and $\vec{n}$ is the direction of the magnetic field $\vec{B}$. We now use the identity

$$e^{-i(\frac{\mu}{v_j\bar{h}})\vec{n}.\vec{\sigma}Bt} = \cos[\frac{\mu}{v_j\bar{h}}\vec{n}Bt] - i\vec{n}.\vec{\sigma}\sin[\frac{\mu}{v_j\bar{h}}\vec{n}Bt]$$

The time evolution of an intial spin $S_j(0)$ in quantum mechanics is given by $S_j(t) = e^{-i\frac{Ht}{\bar{h}}} S_j(0)$. But in our case the electrons are at fixed locations along the path of the transient magnetic field and the only effect of the transient magnetic field is to alignes the spins at different locations it interacts with. Thus we need to study the distribution of spins present in the helical pathway of the transient field. to do this we replace t by $t = \frac{z}{v_j}$, where z is a surface point in the pathway of the transient magnetic field. The appropriate spactial spin aligning evolution operator is $U(z)$, given by,

$$U_j(z) = e^{-i(\frac{\mu}{v_j})\vec{B}.\vec{\sigma}z} = (\cos[(\frac{\mu}{\bar{h}v_j})Bz] - i\vec{\sigma}.\vec{n}\sin[(\frac{\mu}{\bar{h}v_j})Bz], 0 \leq z \leq L$$

We next write $\vec{\sigma}.\vec{n} = \frac{1}{2}$ which is the aligned spin value projected out by the evolution operator. Thus our static helical spin-magnet distribution,$S_j(z)$ is given by,

$$S_j(z) = \frac{1}{2}(\cos[(\frac{\mu}{\bar{h}v_j})Bz_j] - i\sin[(\frac{\mu}{\bar{h}v_j})Bz_j], 0 \leq z_j \leq L$$

It is a helical chain of electron spin magnets. We have already pointed out that the structure has a natural excitation frequency and suggested that this frequency value can overlap with EEG waveform frequencies. For g pulses there will be g static structures given by $S(z) = \sum_{j=1}^{g} S_j z_j$

We have thus shown that memories are static structures labeled by their specific excitation frequencies, so that in the scheme, multiple memories can be stored in multiple static structures each with a characteristic excitation frequencies. Memories thus stored can then be retrieved by a resonance mechanism by signals of appropriate frequency. (sen,2022)

For the biological brain the moving magnetic field of observed action potential, suggested here on theoretical grounds for a mathematical surface, has been measured and has been used to reconstruct an accurate representation the action potential.(Schloss,2016).

Summarizing: a topological way to generate both action potential like and EEG waveform like excitations has been described for a special mathematical surface network that exactly captures the topological connectivity architecture of the brain and has surface has electrons. A dynamical principle that requires the form of the system be respected was introduced. Input signals to the network were defined to be local pinch deformations that had signal specific parameters and they changed the topology of a subunit to that of a sphere. These deformations could be generated by electrical,optical,mechanical or chemical means and a wide variety of excitations could be generated by them, including localized, transient blocking signals. Details of how the dynamical principle converts pinch deformations to soliton and other excitations are discussed elsewhere (sen,2022). Here for completeness we briefly sketch the idea.

To describe surface responses to input pinch deformation signals we need to introduce appropriate functions. For a Riemann surface the appropriate function is the Riemann theta function,(Mumford,1987). But there is a problem. Mathematically a Riemann surface properties depend not on its its size but on its shape. Its shape can be captured by $(6g-6)$ parameters for a genus g surface, however, the Riemann theta function has $g(g+1)$ parameters.(Mumford,1987) For $g > 2$ it has thus more parameters than required. The problem is solved by requiring the theta function satisfy a nonlinear constraint. If the Riemann theta satisfies this constraint then it does represent a Riemann surface. Thus a response to any deformations described by a theta function must satisfy this constraint. In the pinch limit the constraint becomes a set of nonlinear Schroedinger equations that have soliton pulse and other transient excitations as solutions depending on the nature of the pinch deformation. These are thus the responses we seek.

The importance of topology(Nash,1983;Bassett,2020) for exploring global features of the brain is now beginning to be recognized in neuroscience and elsewhere. Topology is the mathematical discipline that studies spaces and structures that do not change under continuous deformations. For example a line and a circle are topologically different but a circle and a square or a triangle are the same. Topological structures are robust. They are global properties of a system. For this reason there is growing interest in using topological methods to identify hidden robust structures present in the vast amount of data available that describe the connectivity architecture of the brain's axon network. This is an important area of current research. Another area of exploration where topological and algebraic geometry methods are being used is to unravel the information contained in brain signals. A few representative references in these growing areas of research are: (Bassett,2020; Curto,2017; Reimann,2017; K.Hess, 2018; M.Marcolli,2019).

The scheme described for signal generation differs significantly from existing methods of signal generation, (Scott,2002; Heimburg,2005; Shrivastava,2020) in several important ways: signals are generated by changing the topology of the surface network and the presence of surface spin half particles play an essential role, and the soliton pulses generated carry with them the surface deformation information that create them. Signals pulses do not carry information in existing approaches and finally in the scheme soliton pulse signals naturally produce EEG waveforms and both of these results hold only if surface electrons are present in the network. These features are absent in other signal generating approaches. It is also essential in our approach that the surface has more than two connectivity surface loops. Without the presence of loops none of our results would hold.

An immediate prediction of the scheme is that memories are magnetic and thus should be affected by external magnetic fields, for instance MRI fields (Krumhout,2012), but not destroyed by them because of their topological stabilty and that memory recall could be improved by low energy low frequency magnetic fields that resonate with the memory structure's natural excitation frequency (Xiauye Cui,2020). It should be noted a large number of memories can be theoretically stored in one pathway since memories are labeled by a continuous frequency. .

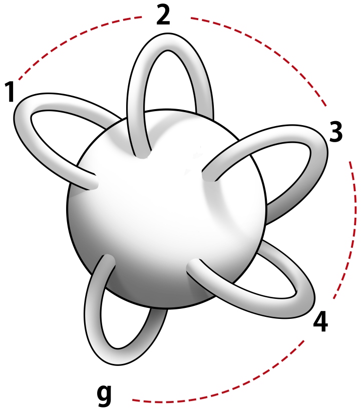

Fig. 1 Genus g surface

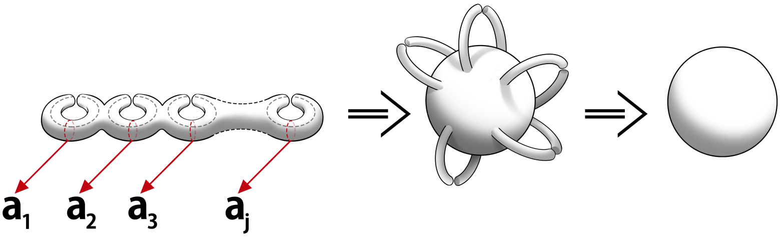

Fig. 2 Degenerate Riemann Surface due to pinching

We can think of a Riemann surface as a ubersurface covering the brain's assembly of three dimensional individual neurons. This is shown in Fig 3.

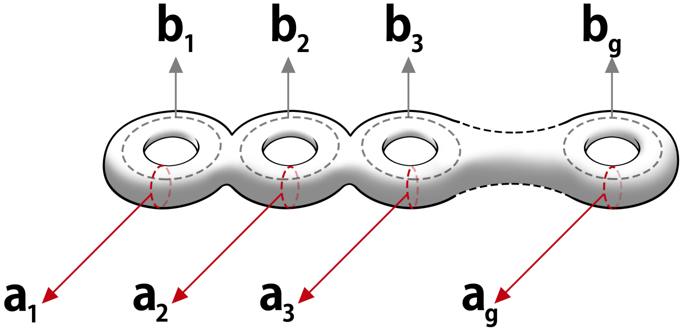

Fig. 3 Marked Riemann Surface.

Results

The nature of surface oscillations can be found by solving an appropriate surface wave equation. The nature of these oscillations, we will show are determined by the topological number W, to be defined shortly. Later we solve the wave equation on the surface of a sphere and find explicit allowed solutions.

Creating Surface waveforms

A wave equation has the structure,

$$\frac{1}{c^2}\frac{\partial^2 \phi}{\partial t^2} - \nabla^2 \phi = 0$$

where ∇^2 is the Laplacian operator. Our first observation is that the dynamical principle requires the solutions of the wave equation to be compatible with the underlying Riemann surface structure. This means that only results that are invariant under conformal transformations are valid, since surface conformal transformations do not change the nature of a Riemann surface. Now a conformal transformations can map a topological sphere to a sphere. Thus we first replace the topological sphere by a sphere solve the wave equation and determine the allowed frequencies and waveform shapes and then note that the frequencies obtained for a spherical surface are invariant under conformal maps, but the Laplacian and waveforms shapes are not. Thus our results for frequencies are in agreement with the dynamical principle but our waveform shapes obtained for a spherical surface are valid to within a conformal transformation. They are approximations.

The wave equation for the surface of a sphere should have a Laplacian with the symmetry of the sphere. This leads to the wave equation becoming a linear second order hypergeometric differential equation (Miller 2010) with three regular singular points (Yoshida,1987). Furthermore we are interested in waveform solutions that fit together on a spherical surface to cover its surface without overlapping as these special waveforms will persist and should be observable special features of the surface oscillations. Thus the topological method of generating action potential like soliton signals remarkably suggest that waveforms that tile the sphere should be co-produced and should be seen. These EEG like waveforms belong to five special frequency bands.

Solutions of the hypergeometric differential equation with three regular singular points are discussed in Appendix A. It is shown that they are determined by certain phases associated with the three regular singular points of the equation The phases form a mathematical group, called the monodromy group. If the group is finite the solutions tile the sphere surface. (Yoshida,1987). This means the waveforms are all alike and they can be placed together to cover the surface of a sphere with no gaps or overlaps.

We identify the three regular singular point locations as three input pinch points where the topological number W enter the spherical surface. If there are more than three input soliton pinch points on the sphere an appropriate generalized hypergeometric equation with more than three singular points is required . Solutions of this equation are also fixed by phases at pinch points, but the solutions are non tiling and are not uniquely determined by the input topological phases(Yoshida 1987). In this case knowledge of the ordering of the input phases is also required to uniquely determine a solution. Hence even though oscillations generated by more than three input phase signals may be present they do not form persistent patterns and hence will appear as a random background of oscillations. For this reason we do not consider them any further but focus on the case where only three soliton signals topological phases are involved. Since our mathematical results are intended to represent events on the surface of neurons we note that there is biological support for considering three input pinch deformations as the number of primary dendrites on a soma, that represent points on the soma where input soliton signals enter a neurons, is between five and seven with a median value of between three and four(Oga 2016,Dharani 2015).

Surface waveform creation by Pinch Deformation Signals

Let us now gather together the ideas discussed. First we define the topological charge W of a soliton pulse. It is a phase which is defined in terms of the discrete labels $(\alpha_i, \beta_i, i = 1, 2, ..g)$ associated with the the two classes of loops (a_i, b_i) shown in Fig 3 that describe of the Riemann surface. These labels mathematically describe surface spin magnets and are called characteristic. Each characteristic $(\alpha_, \beta_i)$ can only take one of two values, namely $(0, \frac{1}{2})$. The definition of W is $e^{iW} = e^{4i\pi \sum_{i=1}^{g} \alpha_i \beta_i}$. The topological number has a simple geometrical meaning. It tells us the pathway points influenced by the soliton since the characteristicβ_i associated a loop b_i while the characteristic α_i is associated with a loop a_i of the Riemann surface (Fig 2).

We now relate the soliton signal phase twists $W_i, i = 1, 2, 3$ at three points to monodromy group phases. We assume that a unit twist associated with a soliton excitation at a pinch deformation point produces a twist of, e^{it} at a regular singular point of the hypergeometric differential equation on Σ_0, the topological sphere created. Then a topological twist W produces a twist $(e^{it})^W = e^{itW}$. This twist is, as discussed in Appendix A, is related to the difference between the characteristic exponents of solutions of the hypergeometric equation at that point. The characteristic exponent values completely determine the nature of a solution of the hypergeoemetric differential equation.(Yoshida, 1987)

Finally a set of characteristics is said to be an even/odd depending on whether $e^{i\pi W} = \pm 1$. For solitons to be produced the characteristic must be odd (Sen,2022). Notice if all the characteristics are set to zero, in the case of no surface spin magnets, the characteristic is even and thus soliton solutions do not exist. We now require that the singular point twist e^{itW} matches topological twist factor $e^{i\pi W}$ of the soliton, which must be (-1). Thus we have the matching condition $e^{itW} = -1$. This fixes the allowed values of t. Possible values of t are $\frac{\pi}{2}, \frac{\pi}{3}, \frac{\pi}{4}, \frac{\pi}{5}$ corresponding to $W = 2, 3, 4, 5$. The monodromy groups generated in this way are of finite order and are hence, by a mathematical theorem, is a tiling solution that is related to the five Platonic solids of antiquity.(Yoshida,1987)

Identifying Special Solutions of the Hypergeometric equation

Explicit tiling soltions of the linear hypergeometric differential equation on a sphere were studied by Schwarz,(Schwarz,1873). Schwarz found 15 algebraic tiling solutions of the second order linear hypergeometric differential equation on the surface of a sphere. Let us give an intuitive reason for this remarkable result. Three facts are helpful.

The first is a property of spherical triangles drawn on the surface of a sphere of radius R with sides that are great circles. Euclid's result that the sum of the angles α, β, γ of a triangle on a plane add up to π radians is now replaced by the result that the sum of angles of a spherical triangle is related to its area in the following way (Wolfram):

$$\alpha + \beta + \gamma - \pi = \frac{A}{R^2}$$

where A is the area of the spherical triangle. Thus the sum of the angles fixes the area of a spherical triangle for a given radius R. Hence given that a sphere of radius R has area $4\pi R^2$ we can find the allowed identical set of triangle that can tile the sphere. This leads to five cases discovered by Plato: the five Platonic solids whose surfaces suitable mapped on to the surface of a sphere tile it using identical subunits.

The second fact, stated before, is that the Laplacian operator necessary to study waves on must have the symmetry of a sphere. This requirement leads to the second order hypergeometric differential equation (Miller 2010).

The third fact, also stated earlier, is that the second order hypergeometric differential equation has two linearly independent solutions with three regular singular points and that these two independent solutions are completely determined by the way they change as they are transported round singular points (Yoshida,1987)(Appendix A). Such a transport produces a phase change of the solution called its monodromy, which is a phase angle. The presence of three regular singular points leads to three angles. These angles, if they have the right set of values, can be represented as the angles of a spherical triangle and that can tile the sphere. This means that these waveforms cover the surface of the sphere without overlapping and thus persist stably. For this to happen the solutions have to have special values for their monodromy phases. The sides of the triangles are the nodes of the waveforms. A mathematical description of the way tiling of spheres and special solutions of the hypergeometric differential equation are related is outlined in Appendix A.

A list of such solutions is available (Vidunas 2008,2009). Examples of tilings are shown in fig 4: Schwarz Triangles

Surface waveform Frequency Estimates

We can give a simple geometric argument to estimate the frequencies of tiling solutions.

The wave like nature of tiling solutions comes from from the fact that they have a periodicity that is induced by the tiling. A solution in one tiling sector has to smoothly join onto the solution in the next sector. This periodicity generates a two dimensional waveform. The size of these two dimensional excitations can be estimated by the area of a tiling segment. If we take the speed of these waves to be approximately tiling independent then we can estimate the frequency of the different waves as being proportional to the inverse of their size.

Let us carry out this frequency estimate for 5 algebraic solutions of Schwarz and then compare our frequency estimates with observed EEG frequencies.

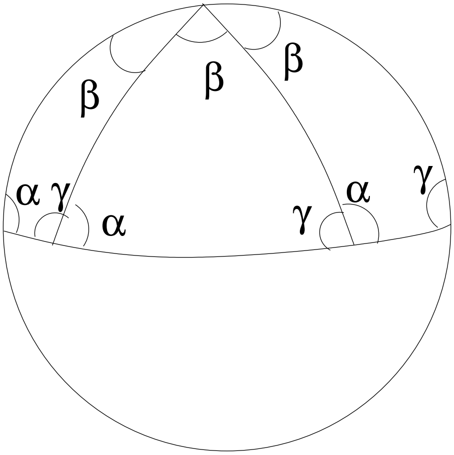

Fig. 4 Schwarz Tiling.

The favorable agreement is noted but we continue to treat these results as mathematical results of our surface network The tilings are described by three angle labels a, b, c that fix the tiling area A, for a spherical triangle, is fixed by by angles of the triangle by the simple formula $\frac{A}{r^2} = a+b+c-\pi$, where r is the radius of the sphere. We tabulate the tiling areas, estimated wave frequencies and state the associated Platonic solid:

Solid	**Area**	**Schwarz labels**
Dihedral	$\frac{p}{n}$	$(\frac{1}{2}, \frac{1}{2}, \frac{p}{n} \leq \frac{1}{2})$
Tetra	$\frac{1}{6}$	$(\frac{1}{2}, \frac{1}{3}, \frac{1}{3})$
Tetra	$\frac{1}{3}$	$(\frac{2}{3}, \frac{1}{3}, \frac{1}{3})$
Cube	$\frac{1}{12}$	$(\frac{1}{2}, \frac{1}{3}, \frac{1}{4})$
Icosa	$\frac{1}{30}$	$(\frac{1}{2}, \frac{1}{3}, \frac{1}{5})$
Icosa	$\frac{1}{15}$	$(\frac{2}{3}, \frac{1}{5}, \frac{1}{5})$

The areas are in units of π. The Schwarz labels are the angles a, b, c written as $a = \frac{\pi}{p}, b = \frac{\pi}{q}, c = \frac{\pi}{s}$. The frequencies are proportional to the inverse of the areas listed. We set the basic frequency equal to one Hertz. We then have the frequency estimates,

Solid	**Size**	**Frequency**	**EEG**	**Predicted**	**Observed**
Dihedral	$\frac{p}{n}$	≥ 2	All waves	$\frac{1}{n}A$	All waves
Tetra	$\frac{1}{3}$	3	delta (.5-3)	$200\mu V$	$200\mu V$
Tetra	$\frac{1}{6}$	6	theta(3-8)	$100\mu V$	$50\mu V$
Cube	$\frac{1}{12}$	12	alpha(8-12)	$50\mu V$	$50\mu V$
Dodaca	$\frac{1}{15}$	15	beta(12-30)	$40\mu V$	$< 50\mu V$
Icosa	$\frac{1}{30}$	30	gamma(30–42)	$20\mu V$	$10\mu V$

We compare our mathematical results with the observed 5 types of global EEG brain wave frequencies, namely, the delta (.5-3 Hz), theta (3-8 Hz), alpha (8-12 Hz), beta (12-30 Hz), and gamma (30-42 Hz) are listed (Liu ,2013). The predicted frequency values setting the base frequency to one Hertz are listed. Thus our estimates roughly agree with observations. This encouraging result is a first step in our identifying the surface network signals as brain signals and the surface oscillations that we are studying as EEG waveforms. For the moment we continue to carry out our mathematical analysis and regard the comparison result as an interesting coincidence. The amplitudes numbers predicted use an input value of $200\mu V$ for delta waves.

We also note that since the Schwarz solutions are solutions of a linear system, a general surface waveform will be a linear superposition of the fundamental set of eigensolutions of the system. This also means that both the amplitude and frequency scales are not fixed by the equation.We next present an estimate of these two parameters using an energy argument that justies our choice of scales.

A Numerical Estimate of EEG frequencies and Amplitudes

Here we give a simple estimate of the Frequency/Amplitude scales and their relationship for EEG waveforms by relating the energy of oscillation of a point on the surface of a sphere and equating it to the maximum voltage oscillation energy. Energy of a point on the surface:$\frac{1}{2}Mv^2 = eV$. The oscillations are coherent. Hence we set $M = 4\pi\rho R^2$. We next set $v^2 = \omega^2\Delta^2$ where ω is the frequency, ρ the average density of the neuron and Δ the maximum amplitude of the surface oscillations. Setting $V_{max} = 100mV, R \approx$ 1mm and $\rho \approx$ 1 gm/cc, we find $\Delta \approx 10^{-5}$cm and the frequency is inversely related to the frequency. Analytic solutions results can be found for allowed tiling waveform frequencies. We can also estimate the speed range of the different EEG waveforms v, since $v = \lambda\omega \approx R{\times}\omega \approx<$ 1cm/s. There will be range of speeds close to this estimate. The higher frequency waves have shorter wavelengths but higher frequencies they should also have speeds in the same range. This is a prediction. These estimate show that frequencies allowed will be in bands as observed EEG waveforms are due to signals from a large number of spheres created by a large number of soliton pulses and no two spheres created will have the same radius and the exactly same density.

Finally we estimate the speed of soliton pulse signals inside the soma by using a conservation of angular momentum argument. Suppose the pulse is moving in the z direction with speed v_s in the soma that has a radius r_s. When it enters the pinched axon hillock its speed is taken to be v_a and the pinched hillock radius is taken to be r_a. Angular momentum conservation requires $v_s r_s = v_a r_a$. Setting $v_a \approx 10^4 cm/s, r_a \approx 10^{-5} cm, r_s \approx 10^{-1} cm$ we get $v_s \approx 1cm/s$, which is compatible with the surface wave speed estimate.

Surface Waveforms: Fractional Legendre functions

We now determine analytic expressions for waveforms and find an explicit formula for their allowed frequencies of tiling solutions for a sub class of tiling solutions that give dihedral, tetrahedral, and cubic tilings. This sub class waveforms can be represented by associated Legendre functions of fractional order, $P_\nu^\mu(z)$. For this class we can write down explicit analytic expressions for the waveforms and find an explicit formula for their oscillation frequencies: the solutions also form a complete set of basis functions (Maier, 2018) so that they can be used to represent any arbitrary square integrable function $f(z)$ on the sphere. Thus, any such function $f(z)$, can be written as,

$$f(z) = \sum_{n=-\infty}^{i=+\infty} c_n P^{\mu}_{\nu_0+2n}(z)$$

where the points z represent arcs on the sphere. From this result and the orthogonality property,

$$\int_{z=-1}^{z=+1} P^{\mu}_{\nu_1}(z) P^{-\mu}_{\nu_2}(-z) = \alpha(\mu, \nu_1)\delta_{\nu_1,\nu_2}$$

we obtain the completeness result,

$$\delta(z - z') = \sum_{n=-\infty}^{n=+\infty} \frac{P^{\mu}_{\nu+2n}(z) P^{-\mu}_{\nu+2n}(-z')}{\alpha(\mu, \nu + 2n)}$$

The dihedral tiling class corresponds to setting $\mu = \frac{1}{2}, \nu = -\frac{1}{2}$. We also have the completeness result,

$$\delta(t - t') = \int d\omega e^{i\omega(t-t')}$$

A more general class of basis functions can also be used for representing functions defined on the sphere rather than along arcs on the sphere. They are the analog of the usual spherical harmonics. We display the ones related to dihedral tiling. We have

$$Y^{-\frac{1}{2}}_{-\frac{1}{2}+2n}(\theta, \phi) = N_{(\frac{1}{2},2n-\frac{1}{2})} e^{-i\frac{\phi}{2}} \sqrt{\frac{8}{\pi \sin\theta}} \cos(2n - \frac{1}{2})\theta$$

where $n = 1, 2, ..$ and $N_{(-\frac{1}{2},2n-\frac{1}{2})}$ is a normalization factor. It is evaluated in the next section. Using this function we can plot EEG waveform-s in two dimensions and display their tiling property.

The completeness property of these solutions and the fact that they are related to solutions of the wave equation on a sphere will now be used to construct a Greens function(Morse, 1953) appropriate for studying space-time dependent modulations of the surface waveforms.

Construction of Greens function for surface wave modulations

The Greens function $G(z, t : z', t')$ satisfies the equation,

$$(\frac{1}{c^2}\frac{\partial^2}{\partial t^2} - \nabla^2)G(z, t : z', t') = \delta(t - t')\delta(z - z')$$

We next replace the right hand side with the delta function representations chosen, with $\mu = \frac{1}{2}, \nu = -\frac{1}{2}$, and use the complete set of dihedral tiling waveforms to write,

$$G(z, z', t - t') = \sum_n \int d\omega \frac{P^{\mu}_{\nu+2n}(z)P^{-\mu}_{\nu+2n}(-z')}{(-(\frac{\omega^2}{c^2}) + \omega_n^2)} \frac{e^{-i(t-t')\omega}}{\alpha(\mu, \nu + 2n)}$$

where $\nabla^2 P^{\mu}_{\nu+2n}(z) = -\omega_n^2 P^{\mu}_{\nu+2n}(z)$ and we have assumed that the Greens function depends only on $(t - t')$. Carrying out the ω integral we get

$$G(z, z', t - t') = i\pi \sum_n (\frac{e^{-i\omega_n(t-t')}}{\omega_n}) \frac{P^{\mu}_{\nu+2n}(z)P^{-\mu}_{\nu+2n}(-z')}{\alpha(\mu, \nu + 2n)}$$

The modulation $m(z, t)$ of an surface waveform due to an input signal $s(t, z)$ can now be calculated. We have

$$m(z, t) = \int dt' \int dz' G(z, t, z', t')s(z', t') \tag{1}$$

The dihedral tiling waveforms, labeled by an index n, have frequencies

$$\omega_n = \sqrt{n^2 - \frac{1}{4}}, \quad n = 2, ..$$

and their waveform shapes are given by the fractional spherical harmonics,

$$Y^{-\frac{1}{2}}_{n-\frac{1}{2}}(\theta, \phi) = N_{(-\frac{1}{2}, n-\frac{1}{2})}\ e^{-i\frac{\phi}{2}} \sqrt{\frac{8}{\pi \sin\theta}}\ \cos(n - \frac{1}{2})\theta$$

where $n = 1, 2, ..$. Thus we have found explicit expressions for surface waveforms and a formula for their allowed frequencies.

We can next relate the frequencies of these waveforms to their amplitude by calculating the normalization factor $N_{(-\frac{1}{2}, 2n-\frac{1}{2})}$. This will determine the way it scales with n and thus establish a relationship between the amplitude and the frequency of a waveform. Using the normalizations of Maier(Maier 2018) for $P^{\mu}_{\nu}(\theta), P^{-\mu}_{\nu}(\theta)$ that can be related their norm $P = P^2 = \int_{\pi}^{+\pi} d\theta \sin\theta P^{\mu}_{\nu}(\theta)P^{-\mu}_{\nu}(\theta)$ can be evaluated. Writing $P^{\mu}_{\nu}(\theta) \rightarrow P\frac{P^{\mu}_{\nu}(\theta)}{P}$, with

$(\mu = \frac{1}{2}, \nu = 2n - \frac{1}{2})$ the n dependence of the amplitude is fixed by P which is,

$$P = \sqrt{\sqrt{\frac{2}{\pi}}\ \frac{\Gamma(\frac{3}{4})}{\Gamma(\frac{5}{4})}\ \frac{(4n+2)}{(2n+\frac{1}{2})(2n+\frac{3}{4})}}$$

Thus a clear inverse relationship between the amplitudes and frequencies is established. Since the dihedral tilings can be used to represent all other tiling solutions, this relationship is valid for all surface waveforms.

There are corresponding set of basis functions for some other tiling waveforms. For, example, for a tetrahedral or octahedral tiling generated surface waveforms, the frequencies are of the form,

$$\omega = \sqrt{(\nu + \frac{1}{2} + 2n)(\nu + \frac{3}{2} + 2n)}$$

with appropriate fixed values for (ν, μ) and (n, m) integers $(0, 1, 2, ..)$ that reflect the symmetry of the tiling, there is a corresponding waveform $Y^{\mu+m}_{\nu+\frac{1}{2}+2n}(\theta, \phi)$. These expressions may be directly used also show the inverse relationship between waveform amplitudes and their frequencies. Thus, for the octahedral tiling case an explicit expression for waveforms is available (Maier 2018). We have,

$$\begin{aligned} P^{\frac{1}{4}+m}_{-\frac{1}{6}+n}(\cos\theta) &= 2^{-2m-3n}\ \Gamma(\frac{3}{4} - m)^{-1}\ (\sin\theta)^{-\frac{1}{4}-m} B_{+}^{\frac{1}{4}+3m+3n} r^{m}_{n}(\frac{B_-}{B_+}) \\ B_{\pm} &= \cos(\frac{\theta}{3}) \pm \sqrt{\frac{4\cos^2(\frac{\theta}{3}) - 1}{3}} \end{aligned}$$

where $r^m_n(\frac{B_-}{B_+})$, for $(n, m) \geq 0$ are Heun polynomials (Ronveaux 1995) of degree $(3n+2m)$ with octahedral symmetry. However we will not consider these cases any further and in all our subsequent work and discussions we will always use the dihedral waveforms to approximate all other tiling solutions and thus represent all surface waveforms.

At this stage we have the mathematical tools required to study the response of the surface waveforms to signals and we have found the waveform oscillation frequencies and their explicit form. We now take the next step and assume that the soliton excitations of our network represent brain signals and our surface oscillations co-produced with any signal created by pinch deformations as EEG waveforms. We thus identify multi-soliton solutions with spike trains, dark soliton solutions that are oscillations on top of a high energy background, with bursts and transient localized excitations that can be generated by pinch deformations, with blocking signals that prevent certain certain brain circuits from functioning, as observed during sleep (Sen,2022). We can then apply the techniques established to analyze observed EEG events.

We carry out such an analysis to discuss the observed sequence of brain EEG events during deep sleep (NREM),namely, K-complexes-Sleep-Spindles and Sharp -Wave Ripples.

Modeling K-complexes-Sleep-Spindles-Sharp Wave Ripples

In NREM sleep delta waves are observed and at intervals of 1-1.7 minutes large sharp spikes, K-complexes, are seen that have amplitudes in excess of 100 mV in the background high amplitude of slow waves and delta waves (1.6-4.0) Hz present. These excitations have duration in excess of 500 ms and are followed by spindle shape oscillations of duration a few seconds of frequency in the range $(10-15)$ Hz, followed by sharp wave ripples (De Gannaro 2003,Ioannides 2019). The events described happen in this order.

We now show that we can interpret this sequence of events as a mechanism of memory consolidation and the transference of memory copies from one region of the brain, possibly the hippocampus, to another region of the brain, possibly the frontal cortex (Buzsaki 1989, 2015) in the framework of our topological surface network . The first step in the sequence of events described is thus assumed to be due to a major transient localized cortical that prevents regions of the brain from receiving or processing information for the period of time. It is a local blocking event. The triggering event should have high voltage, be transient, and localized to an appropriate brain region with a duration in excess of 500 ms. During this period of time other signals cannot proceed in the region where the event has occurred: the region is thus isolated from other signals. Such a blocking transient event, we suggest is responsible for the K-complex modulation of the delta wave that is co-produced with it. A mathematical example of such a transient cortical event which can be created by pinch deformation input signals, exists. Examples are rational breather and peakon solutions(Kalla 2011).

We next suggest that sleep spindles observed reflect the modulation of delta waveforms by the natural frequency excitation of a helical magnetic memory structure (Sen,2022). It was shown that the structure has a natural excitation frequency in the range $(1-30+)$ Hz (Sen 2022).

Finally the memory trace modulation on the high voltage delta waves interact with underlying neurons to produce, by a resonance process, a memory copy carrying burst excitations which, in turn, modulate the delta waveforms co-produced and shows up as sharp wave ripples in the EEG signals. The produced bursts are interpreted as copying and transferring memory information. Because of the extensive nature of the blocking signal the visual and auditory sensory pathways do not respond to these activities.

In earlier work (Sen et al. 2022) it was shown that memories may be stored non-locally as closed static helical magnetic traces $\Delta\vec{B}(x)$ in the pathways traversed by multi-soliton excitations. The non transient trace has a natural excitation frequency which we estimate to be in the range $(1-100)$ Hz.

We now calculate the modulation of a delta waveform potential as it moves over such a magnetic memory trace. In an earlier section we showed that the delta waveform potential was $V(\theta,\phi,t) = Ne^{-i\frac{\phi}{2}}\sqrt{\frac{8}{\pi\sin\theta}}\ \cos(2n-\frac{1}{2})\theta\ e^{i\omega_0 t}$,in terms of spherical polar coordinates, with $\frac{pi}{2} < \theta < \pi$, where N was a normalization constant and $\omega_0 = \sqrt{n^2 - \frac{1}{4}}, n = 2$. Using this expression we can calculate its the gradient $-\nabla V$ which is an electric field that acts on charges e on the tube causing them to move. For a qualitative understanding of this effect, which we show these effects produces spindles, we replace the (θ,ϕ) dependence of $V(\theta,\phi,t)$ by a simpler expression but we retain its theoretically motivated time dependence. Thus we set $V = V_0\sin\theta\sin\phi\cos t$ for the delta waveform, so that $\omega_1 \approx n$. Then $V = V_0 y\cos t$ in Cartesian coordinates and we have,

$$\begin{aligned} E_y &= -\nabla_y V = V_y\cos t \\ m\frac{dv_y}{dt} &= eE_y \\ v_y(t) &= \frac{V_0 e}{m}\sin t \end{aligned}$$

where $V_y = -\nabla_y V$. This moving charge velocitya has an oscillatory frequency and high energy that can excite the helical magnetic trace present and make it oscillate with its natural frequency $\omega_0 = \frac{2\pi v_0^2}{cr_s}$ found in Sen(Sen,2022), where v_0 is the charged soliton pulse speed that led to the magnetic memory trace. Thus creating an oscillating magnetic field,

$$\vec{B}(t,\vec{x},r_s) = B(\vec{x})(\cos(\frac{2\pi v_0^2 t}{cr_s}), r_s\sin(\frac{2\pi v_0^2 t}{r_s}), z = v_0 t),$$

where r_s is the radius of the tube, c the velocity of light in the medium.The natural excitation frequency of the structure is thus $\omega_0 = \frac{2\pi v_0^2}{cr_s s}$. We calculate the modulation of the EEG wave due to this oscillating magnetic by noting that the moving charge interacts with a magnetic field via the electromagnetic Lorentz force (Jackson,1962). For an oscillating charge moving with velocity v_y this interaction force is given by,

$$F_z = \frac{e}{c}Bv_y(t)\cos\omega_0 t$$

producing a modulating potential ΔV given by $F_z dz = -\Delta V$. Thus we have,

$$\Delta V = \frac{e^2 V_0}{mc}B(\sin z)\sin(\omega_0 z)dz,\ 0 \le z \le L$$

where we have used z to parametrize time, setting $B_z = z = v_0 t$ for the helical magnetic memory trace, and we have set $v_0 = 1$. This is a spindle (Fig 5). It carries the helical magnetic memory trace excitation frequency.

Thus ΔV, provides a copy of the excitation frequency of a static memory trace. We now interpret our results in terms of brain excitations. The

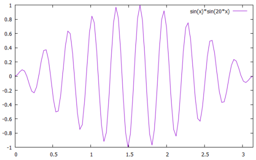

Fig. 5 Sleep Spindle

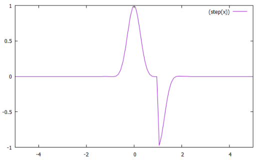

Fig. 6 K Complex

modulation theoretically determined has the shape of a sleep spindle, as $\omega_0 >> 1$.

Observations find that the memory excitation frequencies are in the range $\omega_0 \approx 10 - 15$ Hz which is consistent with our theoretical estimate, discussed earlier, where a estimate of the excitation frequency of a helical spin-magnetic structure was made linking it to the shape properties of the soliton voltage pulses that generated the structure. Memories in the scheme are stored as static structures with frequency labels.

Transient Signals and K-complex

We now give the mathematical details to show how a high energy blocking signal, a transient localized solutions of the non-linear Schroedinger equation can explain a K-complex modulation. Explicit mathematical examples of such transient solutions exist, such as the peakon solution and rational breather solution and their analytic forms are available (Kalla 2011) but, we simplify our analysis by approximating the known analytic solutions for transient excitations, using the following simple expression,

$$\psi(\theta,\phi,t) = \delta(\theta-\theta_0)\delta(\phi-\phi_0)e^{-(\omega_n t)^2}\Theta(t) - \Theta(t-\frac{1}{\alpha})\delta(\theta-\theta_1)\delta(\phi-\phi_1)$$

where $(\theta_1 = \theta_0 + \Delta, \phi_1 = \phi_0 + \Delta)$, and $\Theta(t) = 1, t > 0$ and is zero otherwise, the Heaviside Theta function. The Greens function, for surface dihedral waveforms is given by,

$$\begin{aligned} G(z,z',t-t') &= i\pi(\frac{e^{-i\omega_n(t-t')}}{\omega_n})\ P^{\frac{1}{2}}_{-\frac{1}{2}+2n}(z)P^{-\frac{1}{2}}_{-\frac{1}{2}+2n}(-z') \\ P^{-\frac{1}{2}}_{2n-\frac{1}{2}}(\theta) &= \sqrt{\frac{8}{\pi\sin\theta}}\ \cos(2n-\frac{1}{2})\theta \end{aligned}$$

For our qualitative discussion we drop normalization factors and ignore the spatial oscillations of the waveforms. Then any surface waveform modulation due to a transient localized excitation, can be plotted (Fig 6) using,

$$\begin{aligned} M(t) &= M_1 + M_2 \\ M_1 &= A\frac{1}{\sqrt{n}}e^{-(\omega_n t)^2}\cos\omega_n t, \quad -T < t < +T \\ M_2 &= A\frac{1}{\sqrt{n}} - e^{-(\omega_n (t-2T))^2}\cos\omega_n t, \quad +T < t < +3T \end{aligned}$$

with $\omega_n = \sqrt{4n^2 - \frac{1}{4}}$. For numerical work an appropriate gluing function M_{12} is required. The value of the constant A, has to be chosen.

Thus a K-complex modulation of a EEG delta waveform can be understood as a modulation of the delta waveform by a high energy transient blocking excitation. The transient event is required to have high energy, as the delta waveform co-produced with it and then modulated by it, has high energy. But such transient excitations can theoretically exist with lower energies, ranges and duration. We sketch the possible energies, ranges and durations, that such excitations can have, using brain EEG waveform information. We then suggest that all of these transient excitations should be observed and that they all play a role in the functioning of the brain.

Prediction of Range, Energy and Duration of Blocking Signals

We can predict the duration, range and energies of any one of these theoretically allowed transient excitation that produces K-complex like EEG modulation by linking these parameters to the EEG waveforms that they modulate. Our estimate for duration is, thus, $\tau_n \approx \frac{1}{\omega_n}$, for energy $\approx V$, the voltage amplitude of the waveform, with a range given by the area fraction of a sphere tiled by the waveform. Hence for a delta wave these estimates suggest a duration $\tau_1 \approx \frac{1}{2}$ seconds which is $\approx$ 500 ms (Weigenand 2014). We tabulate the results, listing the n value of an EEG waveform, and the amplitude, in mV, and duration,in ms, of K-complexes EEG modulations created by transient localized excitations.

Waveform	**Wave Number**	**Amplitude**	**Duration**	**Range**
Delta	1	100	500	$\frac{\pi}{2}$
Theta	3	30	100	$\frac{\pi}{3}$
Alpha	6	16	50	$\frac{\pi}{6}$
Beta	10	10	30	$\frac{\pi}{10}$
Gamma	50	2	6	$\frac{\pi}{50}$

We speculated earlier that a person can perhaps initiate transient localized blocking events by chemical means. Our interpretation of the K-complex sequence suggests that it is involved in memory transference and consolidation. This suggests that those that have a greatly reduced number of K-complexes during NREM should not be able to store long term memories. This speculation can be tested.

Plotting EEG waveforms in the dihedral approximation

A representative plot for the theoretically determined delta and theta waveforms are displayed.

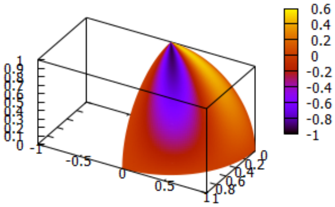

Fig. 7 Theoretical EEG Delta Waveform

The plot shown are tiling solutions, which means that the solutions vanish on the sides of an appropriate spherical triangle. We plot the following expressions,

$$Y^{-\frac{1}{2}}_{2n-\frac{1}{2}}(\theta,\phi) = N_{(-\frac{1}{2},2n-\frac{1}{2})}\; e^{-i\frac{\phi}{2}}\sqrt{\frac{8}{\pi\sin\theta}}\;\cos(2n-\frac{1}{2})\theta$$

where $n = 1, 2, ..$. The angles (θ, ϕ) are spherical polar coordinate angles with ranges $(0 \le \theta \le \pi, -\pi \le \phi \le +\pi)$. To construct tiling solutions that

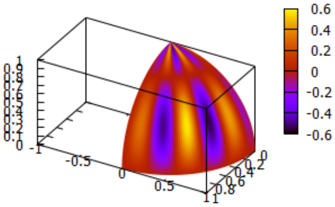

Fig. 8 Theoretical EEG Theta Waveform

vanish on the sides of a spherical triangle the following variable changes are required$\theta \to \theta' = \frac{\theta}{2}, \phi \to \phi' = \frac{\phi}{2n}$ and we require that the solution be periodic in ϕ'. In terms of these variables, the solution becomes,

$$S^{-\frac{1}{2}}_{2n-\frac{1}{2}}(\theta', \phi') = \frac{1}{\sqrt{n}} \cos(n\phi') \sqrt{\frac{1}{\sin 2\theta'}} \cos(2n - \frac{1}{2})2\theta'$$

where the range of the angles are now $(0 \leq \theta' \leq \frac{\pi}{2}, -\frac{\pi}{2n} \leq \phi \leq +frac\pi 2n)$. We check that this solution vanishes when $\theta' = \frac{\pi}{2}$ and when $\phi' = \pm\frac{\pi}{2n}$ which define the three sides of a spherical triangle. Thus we have constructed a tiling solution. To plot this waveform the expression obtained should be multipliede by $\sin(2\theta')$. We have included a normalization factor $\frac{1}{\sqrt{n}}$ which is an approximation of P defined by $P^2 = \int_{\pi}^{+\pi} d\theta \sin\theta P^{\mu}_{\nu}(\theta) P_{\nu}^{-\mu}(\theta)$ with $(\mu = \frac{1}{2}, \nu = 2n - \frac{1}{2})$ the n dependence of the amplitude is fixed by P[28] which is,

$$P = \sqrt{\sqrt{\frac{2}{\pi}} \frac{\Gamma(\frac{3}{4})}{\Gamma(\frac{5}{4})} \frac{(4n+2)}{(2n+\frac{1}{2})(2n+\frac{3}{4})}} \approx \frac{1}{\sqrt{n}}$$

It is clear from this result that the amplitudes are inversely related to frequencies. We list, in tabular form, the frequency and amplitude predictions made for EEG waveforms in this approximation and compared them with observations.

Solid	**Size**	**Frequency**	**EEG**	**Predicted**	**Observed**
Dihedral	$\frac{p}{n}$	≥ 2	All waves	$\frac{1}{\sqrt{n}}A$	All waves
Dihed	$\frac{2}{2}$	1	delta (.5-3)	$200\mu V$	$200\mu V$
Tetra	$\frac{1}{6}$	6	theta(3-8)	$80\mu V$	$50\mu V$
Cube	$\frac{1}{12}$	12	alpha(8-12)	$57\mu V$	$50\mu V$
Dodaca	$\frac{1}{15}$	15	beta(12-30)	$40\mu V$	$< 50\mu V$
Icosa	$\frac{1}{30}$	30	gamma(30–42)	$28\mu V$	$10\mu V$

Memory Recall

We outlined how transient soliton pulses carry signal specific pinch deformation information and can transfer this information along the pathways they travel in the form of a static helical magnetic memory structure that has a characteristic, signal specific excitation frequency, ω_j. A specific memory can thus be recalled by exciting the structure's frequency. It was also suggested that these memory frequencies overlap with those of EEG waveforms. This suggests that memories could be retrieved or recalled by a resonce excitation mechanism. An incoming soliton pulse signal generates EEG waveforms that have a range of oscillations and are determined, as we saw, by the nature of the soliton spin-magnet topological number W. This EEG waveform as it travels will thus only retrieve those memories that have excitation frequencies overlapping with those of the EEG probe frequencies. In the scheme memories are stored as a large collection of static magnetic patterns where each pattern has

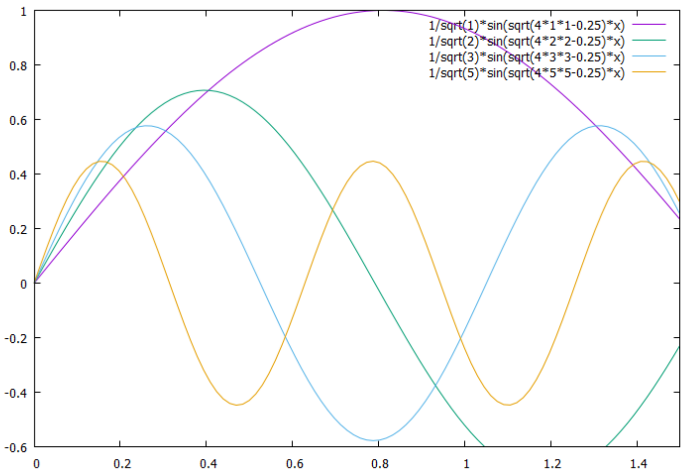

Fig. 9 Theoretical Frequency-Amplitude Plots

its own memory specific excitation frequencies. Thus a given memory can be quickly identified by an appropriate frequency probe. This is a highly parallel processing method.

A similar resonance mechanism is expected to operate during periods of focused attention. During such a period we suggested that appropriate blocking signals are are iniated by a person, possibly by chemical means. The specific set of blocking excitations generate a specific set of EEG waveforms with a specific distribution of frequencies which can then quickly retrieve relevant memories required during such this period. The mechanism described is classical resonance response mechanism but it has similarities with the way a quantum computer works. In a quantum computer the quantum evolution of a state contains in it all possibilities and the process of identifying a specific possibility is in essence done by a resonance mechanism carried out by the overlap of wavefunctions, while here the memory space is a collection of different potential excitation frequencies in an array of static patterns and the probe is a collection of a set of specific frequencies that excites and recalls a specifc set of memories.

Discussion

In this paper we have demonstrated that the form of a special surface network, defined by its topological connectivity and its topological collection of surface spin-magnet patterns, can be used to describe its function as a signal generating and signal processing system. We first proved that a theoretical surface network that exactly captures the topological architecture of any hypothetical brain connectome can be constructed andthat it can be represented by a mathematical Riemann surface. We then sketched how by local topology changing, pinch deformation input signals, all observed brain-like excitations could be generated in the network, provided it had surface electrons. For this to happen the network surface had to be a special Riemann surface associated with a hyperelliptic equation. Our aim to relate the function of the surface to its form was implimented by introducing a dynamical principle which required that all surface distortions: both input pinch topology changing ones as well as the responses of the network to them must respect the mathematical properties of the Riemann surface introduced. This one principle, that the form of the system had to be respected, was enough to derive all of our theoretical results.

Although our network and results are theoretical there were points of contact between assumptions made in the mathematical scheme and the biological brain. Most importantly the form of the network, as defined by its topological connectivity architecture was exactly the same as any hypothetical brain connectome. The surface could thus be viewed as a smooth topological cover of the brain's assembly of three dimensional individual neurons. Generating soliton pulse or other excitations by a subunit of the network required reduced its topology to that of a spherical surface. This surface is expected to be in an excited state and thus have surface oscillations. We showed these surface waveforms had EEG waveform like properties. If the network has less than three closed loops or does not have surface electrons none of our results hold.

A few more points of contact of the mathematical scheme to the biological brain can be listed. They are: It is essential that our surface network has surface electrons. This is plausible as the brain membrane contains positively charged sodium and potassium ions so that negatively charged electrons must also be present perhaps distributed as an irregular lattice. We supposed that pinch deformations can produce excitations. The experimental results of Faisal et al(2005) on the biological brain show that this is true. They pinched axons by reducing their diameter and found that action potentials are generated when the axon radius was below one μm. The third assumption made was that blocking signals can generate EEG waveforms. This was established by Becker (1985) by blocking brain signals by electric means and observing that EEG waveforms were created. Finally we assumed that soliton pulses produce magnetic fields on theoretical grounds. This magnetic field has has been experimentally measured for the brain and used to reconstruct a single action potential spike by Barry et al(2016). Thus basic assumptions of the theoetical scheme are supported by experimental results obtained for the biological brain.

A key result of our earlier work (sen,2022) was that memories regarding signal specific pinch deformation information could be stored in the surface network as static electron spin magnetic structures that have characteristic signal specific excitation frequencies that overlap with EEG waveform frequencies. In view of this result we suggested that EEG waveforms with the right frequency could excite and thus recall specific memories by a resonance mechanism from the multiple collection of memories stored in pathways as static stable structures. Thus this theoretical result could be used to both help identifying the nature of an incoming signal and recall relevant memories required during focused attention (Staresina,2019). We pointed out that this process had similarities with the way a quantum computer functions.

A general prediction of the scheme was that EEG waveforms should have a universal nature, that is, they should have the same structural properties for all creatures that have neuron-synapse architecture, since EEG waves were identified with geometric tiling oscillations on the surface of a sphere. This prediction has experimental support (Bullough,2002, Fingelkurts 2014).

We then used our general linear response formula, (Eq 1) to calculate the modulation of EEG waveforms to understand the sequence of EEG observed in deep NREM sleep that starts with a K-complex, high energy spike. We suggested that the sequence of events is triggered by a major blocking event and that such blocking events of different scales are theoretically expected. We then suggested that if our surface network did provide a mathematical represention of the way the brain generates signals then we speculated that a person could induce blocking events by chemical means. This speculations is testable and it extends the scope of the scheme. For instance, as we noted, it suggest that focused attention is an example of blocking signals operating as unwanted signals during a period of focused attention are not processed. Since blocking signals modulate EEG waveforms in a characteristic way we predict that the occurence of a blocking event will show up in other EEG waveforms as sharp saw tooth like excitations such as the sawtooth wave modulation on theta waveforms observed (Suvadi 2015) before the onset of REM. We expect many sharp waveform structures in gamma waves that indicate the presence of low energy blocking events that are crucial for focused attention.

Thus our results regarding the role played by EEG waveforms in retrieving information, in identifying the nature of incoming signals by a person generating a suitable blocking event by chemical means, in transferring memory copies as interpreted in our account of the K-complex sequence, suggest that EEG waveforms are the muscles of thinking.

The method of EEG waveform like generation proposed here is unconventional. (Nunez 2006a,2006b, DaSilva, 1991, 2010,Jones,2016,Klimeschi,2018). It differs from other approaches in several ways: it treats all EEG waveform generation as excitations co-produced with action potential generation in a uniform way as due to topology change and shows how in such a process the nature of the EEG waveforms are determined by the transference of the soliton pulse spin topology number W to marked points on the topological sphere created during soliton pulse or transient localized blocking excitation generation. The marked points are pinch locations that may be identified as dendrite locations.

In the existing literature, except for the work of Klimeschi where brain body oscillations are analyses to suggest the existence of EEG waveform frequencies, there is no formula for EEG frequencies that relates them to their amplitude neither or links EEG production directly to action potential generation. Our approach and one widely accepted suggestion that EEG waveforms agree on one point, namely dendrite inputs are essential for generating EEG waveforms. In the standard approach EEG waveforms are generated by synchronized dendretic currents loops while in our approach they are generated by topological twists transmitted to the topological sphere created during soliton pulse or transient localized blocking excitation generation. In our approach inputs from solitons to dendrites introduce twist phases, as discussed, that decide the nature of EEG waveforms.

Although our results are mathematically they do seem to capture basic features of observed brain signals and this suggests that the scheme could be a useful way to think about brain signals. We also note that to produce g pulses requires the topological pinching of a genus g subunit. For 10^4 pulses this means including the interaction between approximately 10^4 voltage pulses $V_j(x,t), j = 1, 2, ..g$ as reflected by the nonlinear Schroedinger equation,

$$i\frac{\partial}{\partial t}V_j(x,t) = \nabla_x^2 V_j(x,t) + \sum_{k=1}^{g} s_k V_k^2(x,t)V_j(x,t), j = 1, 2, ..g$$

where $\nabla_x^2 = \frac{\partial^2}{\partial x^2}, s_k = \pm 1$ different choices for s_k produce different excitations. Identifying junction regions with neuron locations this observation also implies the involvement of a large number of neurons in the generation of such a train of soliton pulses.

Declarations

1. This research did not receive any specific grant from funding agencies in the public, commercial or not-for-profit sector.
2. The authors declare no competing financial interests.
3. Availability of data and methods (not applicable)
4. Code availability (not applicable)

Appendix A: Monodromy Groups and Tiling angles

The tiling surface waveforms were shown to be special solutions of the linear hypergeoemetric equation and we described a way to understand how they are co-produce them by pinch deformation excitations. Here we define the monodromy group of the hypergeometric differential equation and explain the link between the monodromy groups and tiling angles required to get the Schwarz solutions.

The hypergeometric equation has two linearly independent solutions and its regular singular points, are chosen to be at $0, 1, \infty$. Each solution has characteristic exponents. Suppose b_0, b_1, b_∞ are the inverses of characteristic exponent differences of the hypergeometric differential equation near the singular points $0, 1, \infty$. We now recall that the hypergeometric equation can be written as,

$$x(1-x)\frac{d^2u}{dx^2} + (c - (a+b+1)\frac{du}{dx} - abu = 0$$

In terms of these parameters we have $\frac{1}{b_0} = \mathsf{1\text{-}c}, \frac{1}{b_1} = \mathsf{c\text{-}a{-}b}, \frac{1}{b_\infty} = \mathsf{a\text{-}b}$, where the terms $\mathsf{1\text{-}c}, \mathsf{c\text{-}a\text{-}b}, \mathsf{a\text{-}b}$ are the characteristic exponent differences of the given hypergeometric equation at its three singular points $x = 0, x = 1, x = \infty$ respectively.

The hypergeometric equation has an underlying group structure. It can be obtained as an eigenvalue equation of the Casimir operator of the Lie algebra $SL(2, C)$ (Miller 2010,Kitaev 2018). The group $SL(2, C)$ represents the symmetry of the sphere. Explicitly the group acts on a a point z of the upper half plane mapping it to a point w by $w = Mz$, where M is a 2×2 $SL(2, C)$ matrix with complex coefficients a, b, c, d as,

$$\begin{aligned} w &= \frac{az + b}{cz + d} \\ ad - bc &= 1 \end{aligned}$$

This is a conformal transformation that maps lines to lines, circles to circles and preserves the angle between two intersecting lines or circles.

The hypergeometric functions also appear as the representaion of the Lie algebra of the group $SL(2, C)$ (Miller 2010) that is the symmetry of the Riemann sphere. The three regular singular points of the hypergeometric equation can be taken to be three points on a sphere. A curved triangle can be drawn on this sphere with these three points as its vertices. The spherical angles between the lines of this curved triangle are chosen to be associated to difference between characteristic exponents of the two linearly independent solutions of the hypergeometric equation at that regular singular point. Thus a solution, described by its characteristics has a geometric representation as a curved triangle on the surface of a sphere.

Fixing the tiling angles

The reason why differences of exponents appear in the analysis can be understood as follows: by analytic continuation (Yoshida 1987) a pair of linearly independent solutions can be extended to all points inside the triangle, the upper half plane and then, by using a reflection principle, (Yoshida 1987) to the lower half plane and thus extended to the entire sphere provided the characteristic exponents of the solutions are special. Such an extension can represent a tiling of the sphere.

Now consider the set $S = (0, 1, \infty)$ of the regular singular points of the hypergeometric differential equation and define $X = C^2 - S$, where C^2 is the two dimensional complex plane and x_0 a point in X. The hypergeometric differential equation has two linearly independent solutions, say u_1, u_2 in the neighborhood of a singular point. If we continue these solutions u_1, u_2 analytically along a curve C in X then we get

$$C_*^t(u_1, u_2) = M(C)^t(u_1, u_2)$$

where $M(C)$ is a non singular two-by-two matrix and C_* represents the analytic continuation of u_1, u_2 along the curve C. The matrices $M(C)$ for different curves forms a representation of the fundamental group of $\Pi(X, x_0)$ and is called the monodromy representation of the differential equation. The monodromy group representation for $\Pi(X, x_0)$ can be constructed from the characteristic exponents of the equations at its singular points. Explicitly if v_1, v_2 are the analytic continuations of u_1, u_2 we can write,

$$\begin{aligned} v_1 &= au_1 + bu_2 \\ v_2 &= cu_1 + du_2 \\ \frac{v_1}{v_2} &= \frac{au_1 + bu_2}{cu_1 + du_2} \\ &= \frac{a\frac{u_1}{u_2} + b}{c\frac{u_1}{u_2} + d} \\ ad - bc &= 1 \end{aligned}$$

Thus if $u_1 \approx z^\alpha, u_2 \approx z^\beta$ near a regular singular point, where α, β are characteristic exponents then the difference of the exponents appear naturally as parameters when we consider ratios of solutions. This is a projective way of studying the solutions. The mondodromy group has the as a linear fractional $PGL(2, c)$ transformation. It is a projective group.The group maps the ratio of appropriate solutions of the hyperheogeometric are real interval in the intervals $(0, 1), (0, \infty), (1, \infty)$. If we consider the strip of the upper half plane with $(0, 1)$ as the real axis then this strip is mapped to the curved triangle joining the point $0, \infty$ and $1, \infty$. The point ∞ is the north pole of the sphere. If such triangle has angles, given by the π(difference between critical exponents) in Schwarz list then by the action of the finite triangle subgroup of $PGL(2, C)$ these triangles tiles the upper half plane. Then by using a reflection principle of Schwarz (Yoshida 1987) this tiling can made to cover the entire sphere provided the spherical triangles have special angle values. Thus special solutions of the hypergeometric equation give a tiling of the sphere. The fact that the group of projective fractional linear transformations $PGL(2, C)$ maps circles and lines to circles and lines and preserves angles is used in the construction described.

The monodromy group $PGL(2, C)$ describes the way twists present at three specified singular points, given by the characteristic exponent differences, fit together. For the hypergeometric differential equation on the sphere this information completely fixes the solutions of the hypergeometric equation(Yoshida 1987).

References

[1] Arberello,E. Sketches of KdV, Contemporary Mathematics,312,9-70,(2001)

[2] Bievins.A.S.,Bassett.D,Topology in Biology,ISBN:978-3-319-70658-0(2020)

[3] Becker,R. and Seldon,G.The Body Electric,New York,Morrow, pages111-113,(1985)

[4] Bullock, T.H.,How do Brain Waves Work? Papers of a Neurophysiologist, Birhauser, Boston.(1993)

[5] Buzsaki,G.,Two stage memory model: a role for noisy brain states, Neuroscience 31(3),551-570(1989)

[6] Buzsaki,G.,Hippocampal sharp wave-ripple: a cognitive biomarker for episodic memory and planning, Hippocampus Oct 25 (10),1073-1085,(2015)

[7] Colgin,L.,et a.,Frequency of gamma oscillations routes flow of information in the hippocampus. Nature, 462, 353-357,(2009)

[8] De Gannaro,L.,Ferrara,M.,Sleep Spindles: an Overview, Sleep Med Rev Oct 7(5) 423-40,(2003)

[9] Curto,C.,What can topology tell us about the neural code?,Bulletin of the AMS,54,63-78,(2017)

[10] Lopez da Silva,F.H.,Neural mechanisms underlying brain waves; from membranes to networks. Electroencephalography and Clinical Neurophysiology,79:81-93,(1991)

[11] Lopez da-Silva,F.,EEG: Origin and Measurements, in EEG-fMRI, Springer Verlag Berlin Heidelberg(2010)

[12] Dharani,K.,Biology of Thought, Academic Press,109-122,(2015)

[13] Faisal,A,White,J,Laughlin,S., Ion Channel Noise Places Limts on the Miniaturization of the Brain Wiring, CurrentBio.15(12)1143-9(2005)

[14] Fingelkurts,Andrew.,Fingelkuts,Alexander.,EEG Oscillatory States: Universality,Uniqueness and Specificity across Healthy-Normal, Alterted and Pathological Brain Conditions, PLOS One9(2),e87507,(2014)

[15] Heimburg, T., Jackson, A., On Soliton Propagation in biomembranes and nerves, PNAS, doi:10.1073/pnas.0503823102 (2005).

[16] Kanari.l,Dlotka.P,Scolamiero.M,Levi.R,Hess.K,Markram,H.,A topological representation of branching neuronal morphologies,Neuroinformatics16,3-13,(2018)

[17] Ioannides,A.,Liu,L.,Kostopoulos,G.,The Emergence of Spindles and K-complexes and the role of the Dorsal Caudal partof the Anterior Cingulate as the generator of K-complexes.,Frontiers of Neuroscience.,doi.org/10.3389/fnins.2019.00814

[18] Jackson,J.D.,Classical Electrodynamics,191,Wiley and Sons,Inc(1962)

[19] Jones,S.,et al.,Neural mechanism of transient neocortical beta hythms: converging evidence from humans, computational modeling, monkeys and mice. PNAS:16041351113,(2016)

[20] Kalla,C., Breathers and generalized non-linear Schroedinger equations as degenerations of algebro-geometric solutions, J.Phys.A: Math.Theor.44 (2011)

[21] Khurgi,J.,Slow ligt in various media,Advanced Optics and

Photonics,Vol2,Issue3,287-318(2010)

[22] Klimeschi,W. (2018) The frequency architecture of brain and brain-body oscillations: an analysis, Eu.J.Neuroscience 48(7),2431-2453

[23] Kitaev,A.,Notes on SL(2,R) representations, arXiv:1711.08169v2,(2018)

[24] Kim,Yoo Sung.,Choi,J.,Yoon,Bo-Eun.,Neuron-Glial Interactions in Neurodevelopment Disorder, Cell,Oct,9(10),2176,(2020)

[25] Nierop,L.,Slottje,R.,vanZandvout,M.,de Vooht,F.,Krumhout,F.,Effect of magnetic strays fields from a 7 Tesla MRI scanner on neurocognition: a double-bind random crossover study, Occuptional and Environmental Medicine,doi:10.1136/oemed/.2011-100468

[26] Landau,L.D,Lifshitz,E.M.,Quantum Mechanics,Elsevier(1977)

[27] Liu,Ning-Han., Recognizing the Degree of Human Attention using EEG Signals for Mobile Sensors, Sensor(Basel)Aug, 10273-10286,(2013)

[28] Maier,R.,Associated Legendre Functions and Spherical Harmonics of Fractal Degree and Order; arXiv:1702.0855v3[math.CA],(2018)

[29] Marcolli,M.,Gamma Spaces and Information,J.Geometric Physics,140,26-55,(2019)

[30] Maya Geva-Sagiv, Yuval Nir.,Local Sleep Oscillations: Implications for Memory Consolidation, Frontiers Nueroscience,13,813,(2019)

[31] Miller,W.,The Lie theory approach to Special Functions. University of Minnesta, November,(2010)

[32] Morse,P and Feshbach, H Methods of Mathematical Physics,791, Chapter7, McGraw-Hill,(1953)

[33] Mumford,D.,Tata Lectures onTheta,Chapter1,3(1987)

[34] Nash,C.,Sen,S.,Topology and Geometry for Physicists, Academic Press,(1983)

[35] Munkres, J., Introduction to Topology, Chapter 12, Prentice Hall International Edition (2014)

[36] Nunez,P.L.,The Neurophysics of EEG(2006a) Second Edition, Oxford University Press

[37] Nunez,P.L and Srinivasan.,A theoretical basis for standing and traveling brain waves measured with human EEG with implications for integrated consciousness. Clinc Neurophysiol, 117(11),2424-2435,(2006b)

[38] Tomofumi Oga, et al.,Basal Dendrites of Layer 3, pyramidal neurons do not scale with change in cortical magnification in Macaque Primary Visual Cortex, (Fig 7), Frontiers Neuron Circuittes 10:74,(2016)

[39] Queenan,B., Ryan, T., Gazzanega, M., Gallistel, C., On the research of time past:The hunt for the substrate of memory, Annals of the New York Academy of Sciences, 1396, 108-125 (2017).

[40] Reimann,M.,Nolte.M,Scolamiero.M,Turner.K,Markram,H.,Cliques-of neurons bound into Cavities Provide a Missing Link between Structure and Function,Frontiers in Computational Neuroscience,Vol 11,art 48(6 pages)(2017)

[41] Ronveaux,A.(Editor)(1995) Heun's Differential Equation, Oxford University Press

[42] Schwarz,H., Crelle Journal,75, 292-335,(1873)

[43] Scott,A.,Neuroscience, A Mathematical Primer, Springer,(2002)

[44] Barry.,J.,Turner,M.,Schloss,J.,Optical magnetic detection of single action potentials using quantum defects in diamond,PNAS,113(49),14133-14138(2016)

[45] Sen,S.,Ryan,T.,Muldowney,D.,Pezzoli,M.,Memory as a Topological Structure on a Surface Network (bioRxiv:doi.org/10.1101/2022.08.01.502331).

[46] Shrivastava, S., Schneider, M., Evidence for two-dimensional solitary sound waves in a lipid controlled interface and its implications for biological signalling, The Royal Society Interface, Vol 11, Issue 97 (2014).

[47] Staresina,B.,Wimber,M.,A Neural Chronometry of Memory Recall,Trendsin Cognitive Sciences,Vol23,No.12(2019)

[48] Suradi,Y.,Sawtooth waves, Neurology;84,e87-e88,(2015)

[49] Vidunas,R.,Transformation of algebraic Gaussian functions; arXiv-087.4808 [mathC.A](2008)

[50] Vidunas,R.,Funkcidaj Ekvacioj,139-180,(2009)

[51] Weigenand,A.,Shellenberger-Costa,M.,Ngo,Hong-Viet,V.,Claussen,J.C.,Characterization of K-complexes and Slow Wave Activity in a Neural Mass Model, PLOS Computational Biology, Nov 13 (2014)

[52] Wolfram MathWorld, Spherical Triangles

[53] Xiaoye Cui,Weicong Ren,Zhiwei Zheng,Juan Li, Repititive Transcrancial Magnetic Stimulation Inproved Source Memory and Modulate Recollection Based Retrieval in Healthy Odler Adults,Front.Psychol,19 June(2020),doi.org/10.3389/fpsyg2020.01137

[54] Yoshida,M.,Fuchsian-Differential-Equations,Friedr.Vieweg-and-Sohn,(1987)

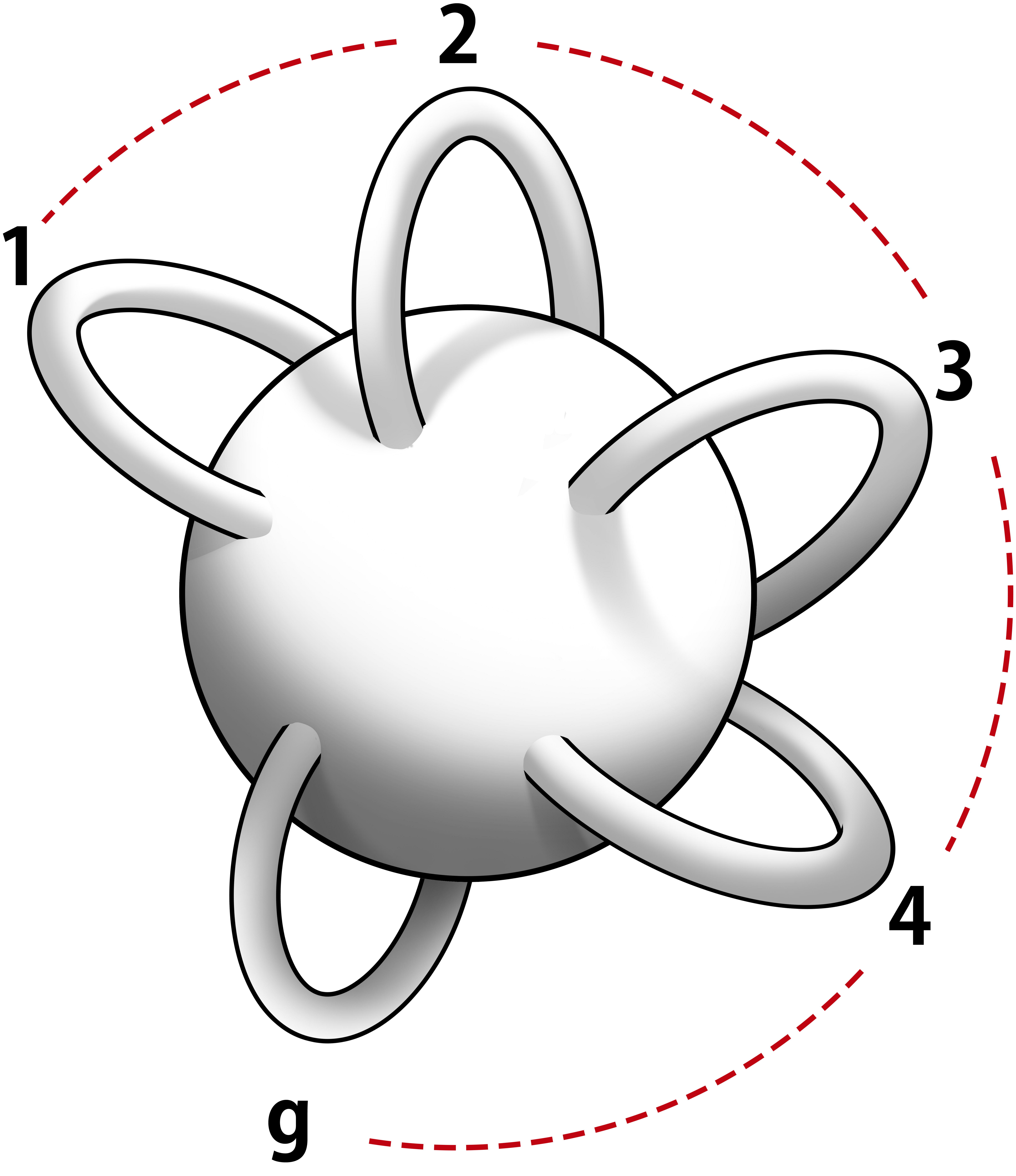

g

b_1
b_2
b_3
b_g
a_1
a_2
a_3
a_g

a_1
a_2
a_3
a_j

a_1
a_2
a_3
a_j

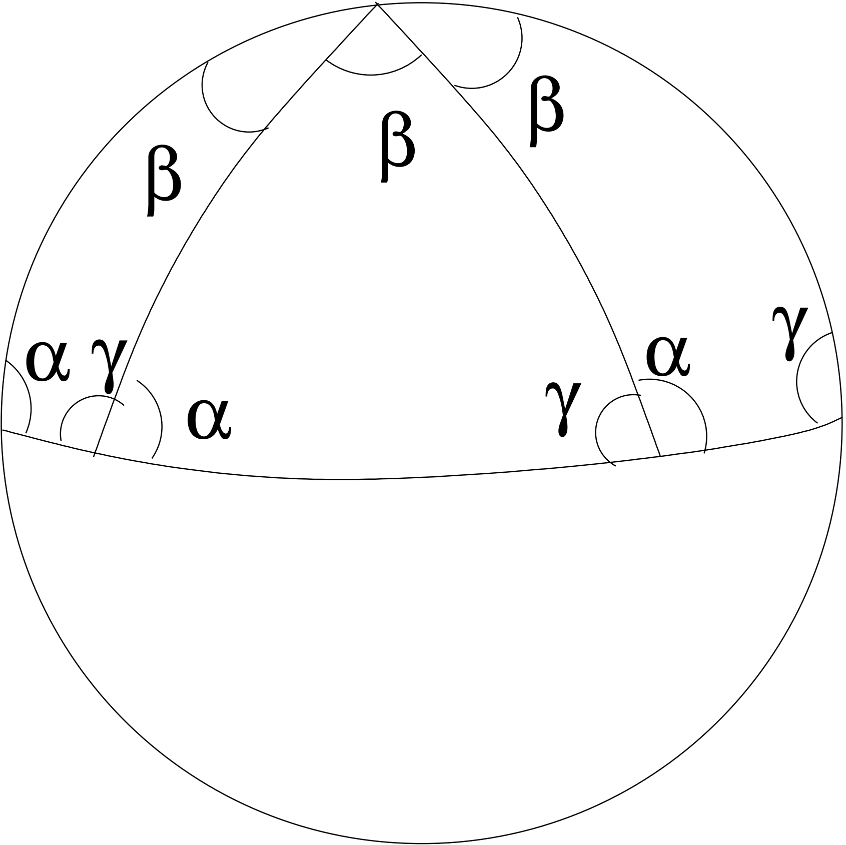
β
β
β
α
γ
α
γ
α
γ
γ

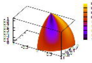

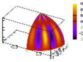
0.4
0.2
0
-0.2
-0.4
1
0

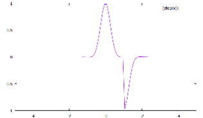
(step(x))
1
0.5
0
0.5
1
4
2
0
2
4

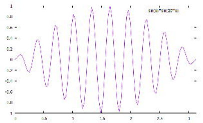
sin(x)*sin(20*x)
1
0.8
0.6
0.4
0.2
0
-0.2
-0.4
-0.6
-0.8
-1
0
0.5
1
1.5
2
2.5
3

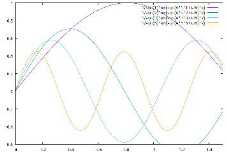
1/sqrt(1)*sin(sqrt(4*1*1.05)*x)
1/sqrt(2)*sin(sqrt(4*2*2.05)*x)
1/sqrt(3)*sin(sqrt(4*3*3.05)*x)
1/sqrt(5)*sin(sqrt(4*5*5.05)*x)
1
0.8
0.6
0.4
0.2
0
-0.2
-0.4
-0.6
0
0.2
0.4
0.6
0.8
1
1.2
1.4